J. Phycol. **42,** 1235–1246 (2006)

DOI: 10.1111/j.1529-8817.2006.00275.x

SEQUESTRATION, PERFORMANCE, AND FUNCTIONAL CONTROL OF CRYPTOPHYTE PLASTIDS IN THE CILIATE *MYRIONECTA RUBRA* (CILIOPHORA)[1]

Matthew D. Johnson[2]

Horn Point Laboratory, Center for Environmental Science, University of Maryland, Cambridge, Maryland 21613, USA

Torstein Tengs

National Veterinary Institute, Section of Food and Feed Microbiology, Ullevaalsveien 68, 0454 Oslo, Norway

David Oldach

Institute of Human Virology, School of Medicine, University of Maryland, Baltimore, Maryland, USA

and

Diane K. Stoecker

Horn Point Laboratory, Center for Environmental Science, University of Maryland, Cambridge, Maryland 21613, USA

***Myrionecta rubra* (Lohmann 1908, Jankowski 1976) is a photosynthetic ciliate with a global distribution in neritic and estuarine habitats and has long been recognized to possess organelles of cryptophycean origin. Here we show, using nucleomorph (Nm) small subunit rRNA gene sequence data, quantitative PCR, and pigment absorption scans, that an *M. rubra* culture has plastids identical to those of its cryptophyte prey, *Geminigera* cf. *cryophila* (Taylor and Lee 1971, Hill 1991). Using quantitative PCR, we demonstrate that *G.* cf. *cryophila* plastids undergo division in growing *M. rubra* and are regulated by the ciliate. *M. rubra* maintained chl per cell and maximum cellular photosynthetic rates (P^{cell}_{max}) that were 6–8 times that of *G.* cf. *cryophila*. While maximum chl-specific photosynthetic rates (P^{chl}_{max}) are identical between the two, *M. rubra* is less efficient at light harvesting in low light (LL) and has lower overall quantum efficiency. The photosynthetic saturation parameter (E_k) was not different between taxa in high light and was significantly higher in *M. rubra* in LL. Lower Chl:carbon ratios (θ), and hence P^{C}_{max} rates, in *M. rubra* resulted in lower growth rates compared with *G.* cf. *cryophila*. *G.* cf. *cryophila* possessed a greater capacity for synthesizing protein from photosynthate, while *M. rubra* used 3.2 times more fixed C for synthesizing lipids. Although cryptophyte plastids in *M. rubra* may not be permanently genetically integrated, they undergo replication and are regulated by *M. rubra*, allowing the ciliate to function as a phototroph.**

Key index words: **ciliate; *Geminigera cryophila*; mixotrophy; *Myrionecta rubra*; nucleomorph; organelle sequestration**

Abbreviations: **CMC, chloroplast–mitochondria complex; HL, high light; LL, low light; LMWC, low-molecular-weight compound; MAA, microsporine-like amino acids; ML, maximum likelihood; NGC, number of genomes per cell; PE, photosynthesis versus irradiance; TBR, tree bisection-reconstruction**

Myrionecta rubra (=*Mesodinium rubrum*) (Lohmann 1908, Jankowski 1976) (Mesodiniidae, Litostomatea) is a photosynthetic ciliate with a widespread global distribution and is known to cause recurrent red-water blooms in numerous regions (Taylor et al. 1971, Lindholm 1985). Photosynthetic measurements during *M. rubra* blooms have been among the highest primary production rates ever measured (Smith and Barber 1979). Blooms of *M. rubra* can be massive in scale and highly dynamic in their water column position (Ryther 1967, Crawford et al. 1997). *M. rubra* feeds on cryptophyte algae (Gustafson et al. 2000) and possesses plastids, mitochondria (Taylor et al. 1969, 1971), and nuclei (Hibberd 1977, Oakley and Taylor 1978) of cryptophyte origin.

Unlike most plastid-retaining ciliates, *M. rubra* is able to grow phototrophically for long periods without feeding on new prey and has the ability to synthesize chl (Gustafson et al. 2000, Johnson and Stoecker 2005). Despite the fact that it ingests cryptophyte algae, *M. rubra* is generally considered a functional phototroph as most of the ingested cryptophyte organelles and cytoplasm appear to be retained in membrane-delineated compartments (Taylor et al. 1969, 1971) rather than being digested. Recent estimated C

[1]Received 21 March 2006. Accepted 10 July 2006.

[2]Author for correspondence and present address: Institute of Marine and Coastal Sciences, Rutgers University, 71 Dudley Road, New Brunswick, NJ 08901-8521, USA. E-mail johnson@marine.rutgers.edu.

budgets for *M. rubra* suggest that ingested prey C accounts for negligible C growth requirements compared with photosynthesis (Yih et al. 2004, Johnson and Stoecker 2005). In contrast, most kleptoplastidic protists form recognizable food vacuoles from algal prey, have been shown to be capable of heterotrophy, and generally do not sequester other prey organelles (Lewitus et al. 1999). Because *M. rubra* is capable of predominantly phototrophic growth and pigment synthesis, it falls into a special functional category (Gustafson et al. 2000).

While many protists are thought to sequester chloroplasts from algal prey, relatively few studies have been conducted to evaluate plastid performance and function in "host" cells. Most studies that have evaluated carbon metabolism in kleptoplastidic protists have focused on oligotrich ciliates. Plastid-retaining oligotrich ciliates have been shown to possess high cellular photosynthetic rates (Stoecker et al. 1988), high plastid turnover rates (Stoecker and Silver 1990), and appear to use photosynthate predominantly for respiration (Putt 1990). Kleptoplastidic dinoflagellates, while widely documented, are less well understood in regards to their physiology. *Gymnodinium gracilentum* and *Pfiesteria piscicida* can acquire photosynthate from kleptochloroplasts for up to a week; however, the amount is insufficient to cover their entire C budget (Skovgaard 1998, Lewitus et al. 1999). Recent research with *M. rubra* has shown that plastids remain functional for up to 8 weeks in low light (LL), while growth and pigment synthesis slowly become negligible (Johnson and Stoecker 2005).

In order to demonstrate that *M. rubra* retained plastids from *Geminigera* cf. *cryophila* (Taylor and Lee 1971, Hill 1991) we designed a quantitative "real-time" PCR Taqman assay for the nucleomorph (Nm) small subunit (SSU) rRNA gene of *G.* cf. *cryophila*. The assay was used to quantify Nm SSU rRNA gene content by normalizing to *G.* cf. *cryophila*–only standards, yielding an estimate of *G.* cf. *cryophila* Nm number (=plastid number) per *M. rubra* cell. The Nm SSU rRNA gene was used because the Nm is always present in cryptophyte plastids, including those in *M. rubra* (Taylor et al. 1969, 1971, Hibberd 1977), and the Nm SSU gene has variable regions with high substitution rates and insertions referred to as nonalignable regions (Hoef-Emden et al. 2002) that allow species-specific identifications. Herein we contrast plastid function and performance in the cryptophyte *G.* cf. *cryophila* with plastid function and performance in its organelle-sequestering predator, *M. rubra*.

METHODS

Culture and experimental conditions. *M. rubra* (CCMP 2563) and *G.* cf. *cryophila* (CCMP 2564) were isolated from McMurdo Sound, Antarctica, from a nutrient-enriched sample of sea ice and water collected in January 1996 (Gustafson et al. 2000). Cultures were grown in 1 L glass flasks with 32 PSU F/2-Si media (Guillard 1975), at 4° C. In preparation for this experiment, cultures were allowed to acclimate to four 24 h light regimes at 90, 75, 25, and 10 μmol photons $\cdot m^{-2} \cdot s^{-1}$ for more than 3 months, while receiving biweekly additions of F/2 media and prey. We were unable to grow *M. rubra* at 10 μmol photons $\cdot m^{-2} \cdot s^{-1}$, due to accumulation of free-living prey. This was probably due to lower ingestion and growth rates by *M. rubra*, and as a result, no data were available from this light intensity for the ciliate. All cell attribute and photosynthesis measurements were made on cells in mid to late log phase. Prey concentrations were checked in *M. rubra* cultures before experimental measurements to verify they were at "background" levels (i.e. <50 cells $\cdot$ mL^{-1}), while *M. rubra* cell concentrations during experimental measurements were above 10,000 cells $\cdot$ mL^{-1}. Experimental treatments each had three replicates unless otherwise noted. Growth rates were estimated during the exponential portion of the growth phase using $\mu\ (\text{div} \cdot \text{d}^{-1}) = (\log_2(n_1 n_0))t_1 - t_0$, where n represents cell concentrations at the beginning and start of the exponential growth phase. All cultures were fed about 2 weeks before experimental measurements, using prey acclimated to the same growth conditions.

DNA extraction, PCR amplification, and DNA sequencing. Cultures of *M. rubra* ($\sim 3 \times 10^4$ cells $\cdot$ mL^{-1}) and *G.* cf. *cryophila* ($\sim 1 \times 10^5$ cells $\cdot$ mL^{-1}) were centrifuged in 50 mL centrifuge tubes at 4° C and 4000*g* for 10 min. The Plant DNA Extraction Kit (Qiagen, Valencia, CA, USA) was used, and the manufacturer's protocol was followed. The PCR was conducted using 1 × PCR buffer (TaqPro, Denville, Metuchen, NJ, USA), 0.2 μM of a deoxynucleoside triphosphate (dNTP) mixture (Bioline, Randolph, MA, USA), 0.25 mg/mL BSA (Idaho Technologies, Salt Lake City, UT, USA), 3 mM $MgCl_2$ (Life Technologies, Rockville, MD, USA), 0.4 μM primers (each), and 0.6 U Taq DNA polymerase (Denville), combined with 10–20 ng of genomic DNA from cultures in a volume of 25 μL. The following general eukaryotic primers for SSU rRNA were used to amplify the gene from conserved regions: 4616, 4618 (Medlin et al. 1988, Oldach et al. 2000), 516, and 1416 (Johnson et al. 2004). The PCR conditions were as follows: an initial 3 min 95° C melting step, 40 cycles of 30 s at 95° C (melting), 30 s at 55° C (hybridization), and 70 s at 72° C (elongation), followed by a final 10 min 72° C elongation step. Products were then cloned using a TOPO TA cloning kit (Invitrogen, Carlsbad, CA, USA), following the manufacturer's instructions. Colonies were isolated and gene products reamplified with PCR using manufacturer supplied vector primers. Cloned PCR products were sequenced in both directions using the above gene-specific primers and the BigDye terminator kit (Perkin Elmer, Boston, MA, USA). All sequencing was conducted using an Applied Biosystems (ABI, Foster City, CA, USA) 377. Species-specific SSU rDNA primers (Operon Technologies, Huntsville, AL, USA) were designed for all sequences identified from sequencing the SSU rDNA clone library, and all sequences were generated at least 10 times.

Phylogenetic analysis. Contingent sequences were generated using Sequencher (Gene Codes Corp., Ann Arbor, MI, USA) and added to sequences obtained from GenBank. All alignments were created using the Clustal X algorithm (Thompson et al. 1997), and ambiguously aligned regions of the Nm alignment, found in highly variable regions, were excluded by eye in MacClade 4.05 (Maddison and Maddison 1992). An alignment matrix was constructed of diverse cryptophytes and red algae (out-group) for the Nm analysis (1842 characters), while the nuclear SSU rRNA analysis (1829 characters) included cryptophyte and glaucocystophyte (out-group) taxa. Both are available upon request.

In order to run a maximum likelihood (ML) analysis, we first ran a distance analysis to estimate base frequencies (Nm = A: 0.2653, C: 0.1993, G: 0.2488, T: 0.2866; nucleus [Nu] = A: 0.2573, C: 0.2030, G: 0.2664, T: 0.2733) and GTR

substitution rates (Nm = A–C: 1.665, A–G: 6.018, A–T: 2.219, C–G: 2.188, C–T: 8.514, G–T: 1; Nu = A–C: 0.9447, A–G: 1.755, A–T: 0.8768, C–G: 1.184, C–T: 3.434) using stepwise addition and 25 × random addition heuristic searches with tree bisection-reconstruction (TBR). These values were then used to run an ML analysis using stepwise addition with 1 × random addition heuristic searches and TBR, Γ-corrected (Nm = 0.4317; Nu = 0.6326), and pinvar (Nm = 0.5179; Nu = 0.4364). The ML analyses included 15 (Nm) and 16 (Nu) in-group taxa and two out-group taxa for both analyses. ML tree scores of 7686.45 and 7339.95 were found for the Nm and Nu analyses, respectively. Bootstrap analysis was performed on all trees, with the respective initial model, on 100 resampled data sets using stepwise addition and a 1 × random addition heuristic search. All phylogenetic analyses were conducted in PAUP* version 4.0b (Swofford 1999).

Quantitative PCR. Primers and probes for conducting quantitative real-time PCR targeting the SSU gene of *M. rubra* and *G*. cf. *cryophila* Nm were designed by eye in MacClade and ordered from Operon. All probes and primers were tested for appropriate melting temperatures and complications due to secondary structures using Primer Express 1.0 (ABI). Primers and probes were added at a final concentration of 0.2 and 0.3 μM, respectively. Taq polymerase (TaqPro) was used at final concentration of 0.1 U/μL (Denville); $MgCl_2$ at a final concentration of 4 mM (Life Technologies); a dNTP mixture, each at 0.2 mM (Bioline); PCR buffer was at a final concentration of 1 × (Denville). For the *G*. cf. *cryophila* Nm assay, the forward primer (FP) TMTA_Nm-F (CCGAGGC TCTTTGGTTAGACT), reverse primer (RP) TMTA_Nm-R (GCCATGCGATTCGGTTAGT), and probe (P) TMTA_ Nm-P (6-FAM-TCGCCATTCATCACCTGATGGAAG-TAM-RA) were used, while for the *M. rubra* nuclear assay, FP MR-F (ACGTCCGTAGTCTGTAC), RP MR-R (ATGATCC TAAGACGAGAAACTTA), and P MR-P (FAM-GAATGCG GTAGTTTCTGCAGTCACTC-BHQ1) were used. All real-time PCR was conducted in a Smart Cycler (Cepheid, Sunnyvale, CA, USA), using 25 μL reaction tubes. A standard curve for the Nm SSU rRNA gene was created using a dilution series of cells from the *G*. cf. *cryophila* culture. The resulting cycle numbers were then plotted against cell number, and an equation was obtained using a best-fit linear regression ($y = -1.3854\,\mathrm{Ln}(x) + 36.316$; $r^2 = 0.987$). A standard curve was also obtained using serial dilutions of *M. rubra* ($y = -1.5863\,\mathrm{Ln}(x) + 28.576$; $r^2 = 0.999$). *M. rubra* cultures were grown at 45 μmol photons $\cdot\,m^{-2}\cdot s^{-1}$ in the absence of prey for ~2 weeks and DNA was extracted on days 2, 5, 9, 12, and 15 for qPCR. Using the standard curves, Nm SSU rRNA gene content was normalized to that of *M. rubra* nuclear SSU rRNA gene content. Assuming an average of one plastid per "Nm containing compartment" (i.e. periplastidal compartment) (Gillott and Gibbs 1980), this can be expressed as plastid number per *M. rubra* cell (PNC).

TEM. Cells were fixed with 4% paraformaldehyde (EMS, Hatfield, PA, USA), 2% glutaraldehyde (Sigma, St. Louis, MO, USA), 0.05 M cacodylic acid (EMS), and 0.1 M sucrose (Sigma) for 2 h at 4° C; centrifuged (1700 *g*, 10 min); washed with 0.05 M cacodylic acid and 0.1 M sucrose buffer; and washed again with 0.05 cacodylic buffer. Cells were then postfixed with 1% osmium for 3 h (EMS). Dehydration was in ethanol, and embedding in Spurr's resin. Embedded cells were thin sectioned, placed on a copper grid, and stained with uranyl acetate (EMS) and lead (EMS) for TEM viewing on a JEOL (Peabody, MA, USA) 1200-EX.

Cellular attributes. Cell volume was determined by measuring cell length and width using a ocular micrometer on a Nikon Eclipse (Nikon Instruments Inc., Lewisville, TX, USA) inverted microscope at ×100 magnification, for at least 30 cells per replicate and time point. Cell volume was calculated using $V\ (\mu m^3) = (\pi 6^{-1})w^2L$, where w is the cell width, and L the length. Cell concentrations were enumerated by counting gluteraldehyde-fixed (1% final concentration) cells at ×100 magnification on a Nikon Eclipse standard microscope, equipped with a fluorescent light source, and Nikon filter sets EF-4 B-2A (exciter filter 450–490 nm, dichromatic beam splitter [DM] 500 nm, barrier filter [BA] 515 nm). Chl *a* was extracted by filtering culture aliquots onto a GF/C filter and incubating overnight in 90% acetone at −20° C. Chl *a* concentrations were determined using a Turner Designs (Sunnyvale, CA) model 10-AU fluorometer.

Light absorption measurements. Cell cultures were filtered onto Whatman GF/F filters in order to measure total particulate absorption (a_{tot}) spectra (Kishino et al. 1985) using a Shimadzu UV-VIS 2401 dual-beam spectrophotometer (Shimadzu, Columbia, MD, USA), equipped with a Shimadzu IRS-2100 integrating sphere. Detrital absorption (a_d) was determined by scanning the same filter following pigment extraction with methanol and 10% bleach (to remove phycobilins). Pigment absorption (a_p) was then determined as $a_{tot} - a_d$. Owing to incomplete removal of cryptophyte phycobilins, a portion of the detrital scan was removed, and remaining data used to fill in the gap by interpolating a power function curve. A β-correction factor ($a^{(\mathrm{suspension})} = 0.59a^{(\mathrm{filter})}$, $r^2 = 0.94$) was determined for the Shimadzu IRS-2100 (Adolf et al. 2003).

Photosynthesis (^{14}C) measurements. Photosynthesis versus irradiance (PE) measurements (Lewis and Smith 1983) were made during exponential cell growth phase, at 4° C using a photosynthetron (CHPT Manufactures Inc., Georgetown, DE, USA) connected to a chiller. Culture aliquots were removed and kept on ice around midday, and $NaH^{14}CO_3^-$ (ICN, Irvine, CA, USA) was added to a final activity of 1 μCi/mL^{-1}. At $t = 0$ controls were taken by adding 2 mL of labeled culture immediately to a vial with 200 μL of formalin (Sigma) and used later for subtracting background levels of ^{14}C activity. Samples for total activity were collected by adding 100 μL of sample to 200 μL of β-phenylethylamine (Sigma). Background and total activity controls were then placed in the dark at 4° C overnight. The ^{14}C spiked culture (2 mL) was then added to 7 mL scintillation vials, on ice, and immediately transferred to the chilled photosynthetron block. A total of 15 vials was used for each replicate PE assay and incubated for 30 min at constant irradiance between 0 and 800 μmol photons $\cdot\,m^2\cdot s^{-1}$. At the end of the incubation, the vials were acidified with 500 μL 6 N HCl to remove unincorporated ^{14}C and placed on a shaker overnight at room temperature. In order to determine the ^{14}C activity of the vials, 4 mL of Ultima Flo AP (Perkin Elmer) scintillation cocktail were added to the background control and light-exposed vials, while 5 mL were added to the total activity vials. All ^{14}C incorporation and control activities were determined using a Tri-Carb 2200CA liquid scintillation counter (Packard Bioscience, Meriden, CT, USA). Photosynthetic rates were determined using analytical methods described by Parsons et al. (1984), and PE data was normalized to hourly rates and either cell or chl concentrations. Curve fitting for PE data was conducted in Sigma Plot (SPSS software, Chicago, IL, USA) using an equation based on Platt et al. (1980): photosynthesis $(P) = P_0 + P_s[1 - \exp(-E\alpha/P_s)]\exp(-E\beta/P_s)$, where P_0 is the y-intercept, P_s is the maximum potential rate of photosynthesis, α is the initial light-limited slope of the PE curve, E is the irradiance, and β is the slope of the photoinhibition region of the curve. From the curve-fitted data, α, P_{max} (maximum rate of photosynthesis), I_k (photosynthesis-saturating light irradiance $[I_k] = P_{max}/\alpha$), and β were determined. P_{max} and α rates are presented both as cellular (e.g. $P^{cell}_{max} = P_{max}\cdot mL^{-1}/cells\cdot mL^{-1}$) and chl (e.g. $P^{chl}_{max} = P^{cell}_{max}/chl\cdot cell^{-1}$) normalized rates in this study (Table 1).

TABLE 1. Abbreviations and photosynthetic parameters throughout the text.

Symbol	Definition
Nm	Nucleomorph
μ	Growth rate (d^{-1})
a^{chl}	Chl *a*–specific spectral absorbance
$a(p)^{chl\ 335}$	Chl *a*–specific spectral absorbance at 335 nm
F_v/F_m	Variable fluorescence (dimensionless)
P^{cell}_{max}	Cellular photosynthetic capacity (pg C · cell^{-1} · h^{-1})
P^{chl}_{max}	Chl *a*–specific photosynthetic capacity (pg C · pg chl a^{-1} · h^{-1})
P^{c}_{max}	C-specific photosynthetic capacity (pg C · pg C^{-1} · h^{-1})
α^{cell}	Cellular photosynthetic efficiency [pg C · cell^{-1} · h^{-1} (μmol photons · m^{-2} · s^{-1})$^{-1}$]
α^{chl}	Chl *a*–specific photosynthetic efficiency [pg C · pg chl a^{-1} · h^{-1} (μmol photons · m^{-2} · s^{-1})$^{-1}$]
E_k	Light saturation parameter from PE curve (μmol photons · m^{-2} · s^{-1})
θ	Chl *a*:C ratio

Variable fluorescence measurements. A pulse amplitude modulated (PAM) fluorometer (PAM-101, Heinz Walz, Effeltrich, DEU) was used with a high sensitivity detector. Ten to 20 mL of culture were placed in a glass test tube, and the tube was illuminated using irradiance from a 150 W xenon lamp and filtered with Schott (Elmsford, NY, USA) long-pass filters. Steady-state *in vivo* chl fluorescence (F_s) of cells was measured during illumination with actinic irradiance. At 1 min intervals a saturating pulse (400 ms duration) was applied to obtain a maximum yield (F'_m). The relative efficiency of excitation energy capture by PSII was calculated as $(F'_m - F_s)/F'_m$ yielding the parameter F_v/F_m (Table 1).

Carbon partitioning measurements. *M. rubra* or *G.* cf. *cryophila* cells were labeled with 0.1 μCi/mL^{-1} $NaH^{14}CO_3^-$ for 24 h at culture growth conditions. For analysis of *M. rubra* cultures, care was taken not to use cultures with free-living cryptophyte prey present. After incubations, cells were gently filtered onto GF/C filters and placed in a glass 20 mL scintillation vial and acidified with 0.1 mL of 10% HCl and heated at 55° C until dry, then stored at −20° C until extraction. Filters were processed for biochemical partitioning of carbon fixation, using the serial extraction method adapted from Morris et al. (1974). Filters were folded in half and placed in a microtube with 1 mL of chloroform (lipid fraction; Sigma), vortexed, and placed on ice for 10 min. Tubes were spun at 10,700 *g* for 5 min (for all steps) and the supernatant was decanted. This extraction was repeated with an additional 0.5 mL of chloroform. Filters were then extracted with methanol (small molecular weight fraction; Sigma), vortexed, and placed on ice for 10 min, centrifuged, and the supernatant was decanted. A second methanol wash step was repeated with 0.5 mL. Filters were then extracted with 1 mL of 5% trichloric acetic acid (TCA; Sigma) at 90° C for 1 h. Tubes were vortexed, centrifuged, and the supernatant was decanted. Filters were then washed with 0.5 mL of cold TCA, yielding TCA-soluble (polysaccharide) and TCA-insoluble (protein) fractions. Various cell fractions were processed for carbon fixation partitioning by adding scintillation fluid and processing the samples as described above for PE curves.

Data analysis. Statistical analysis of cell attributes and PE parameter data were conducted using the mixed model ANOVA and multiple regression options in SAS/STAT 9.0 (SAS Institute Inc., Cary, NC, USA), and $P<0.05$ as a level of significance. Comparisons for ANOVAs between means were made between treatments (HL vs. LL) and over time using Tukey's Studentized range (HSD) test.

RESULTS

Nm and nuclear SSU RNA cryptophyte gene analysis. In order to identify the phylogenetic origin of plastids in our *M. rubra* culture, DNA sequences were determined for the SSU rRNA gene of the plastid Nm in both *M. rubra* and the prey cryptophyte. Identical sequences were obtained from both the *M. rubra* culture and the cryptophyte-only culture. ML analysis (Fig. 1) revealed that this Nm sequence is most closely related to *G.* cf. *cryophila* (strain CS-138) (four substitutions, five indels per 1783 bp), with 98% bootstrap (BS) support. Sequences identical to *M. rubra* SSU rRNA sequences published previously (Johnson et al. 2004) were also found. The cryptophyte prey culture has been referred to in the past as *Teleaulax acuta* based on microscopic examination (Gustafson et al. 2000, Johnson et al. 2004, Johnson and Stoecker 2005). While no *T. acuta* Nm sequence was available in GenBank for comparison, a nuclear SSU rRNA *T. acuta* (strain = MUCC088) sequence was used to help clarify the identity of the cryptophyte culture. ML analysis revealed that on a nuclear level the cultured cryptophyte was more closely related to *G.* cf. *cryophila* (three substitutions, two indels per 1777 bp) than *T. acuta* (18 substitution, five indels per 1777 bp), with 100% BS support (Fig. 2).

In order to demonstrate that our *M. rubra* culture possesses plastids from *G.* cf. *cryophila*, quantitative PCR was conducted for the *G.* cf. *cryophila* Nm sequence. The *M. rubra* culture used for this experiment had not been fed for 3 weeks and no free-living prey were detected using microscopy during the entire time. The number of Nucleomorph genomes per cell (NGC,~PNC) during the first 10 days was between 9.3 and 10, during which time *M. rubra* cell numbers nearly doubled (Fig. 3). At the end of 15 days the cell population had undergone 1.32 divisions and NGC was 8.2 ± 0.1 (Fig. 3). While these NGC numbers are slightly greater than measured *M. rubra*:*G.* cf. *cryophila* chl *a* per cell ratios for this experiment (varying between 6.8 and 7.9 over 15 days), it is possible that chl content of sequestered plastids in *M. rubra* is regulated differently than in *G.* cf. *cryophila*.

Growth and cellular characteristics. Cultures of *Geminigera* cf. *cryophila* had significantly higher growth rates than *Myrionecta rubra* at all irradiance levels (Table 2). Growth rates for *G.* cf. *cryophila* decreased with decreasing irradiance, while *M. rubra*

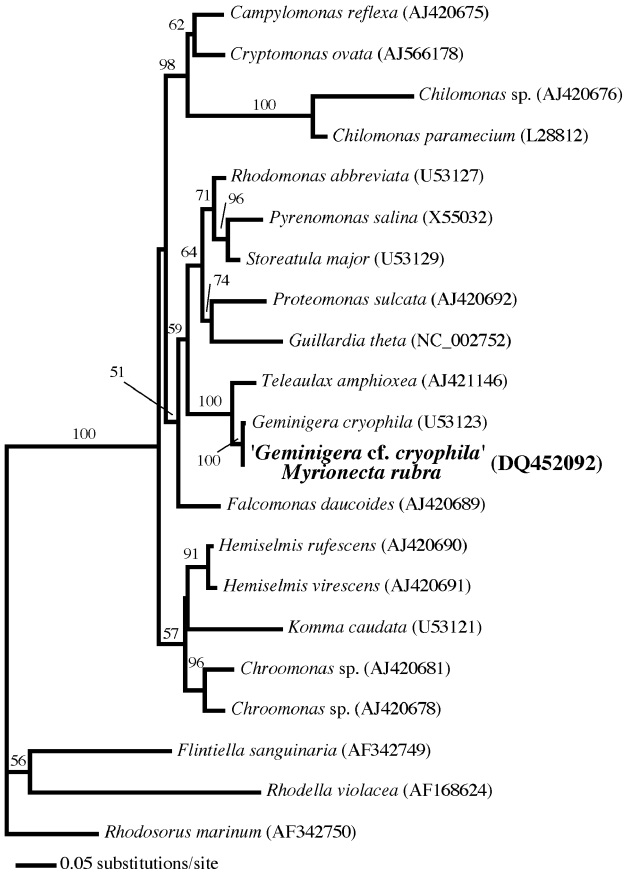

FIG. 1. Phylogenetic analysis of cryptophyte nucleomorph (Nm) small subunit rRNA gene for *Geminigera* cf. *cryophila* and *Myrionecta rubra* using a gamma-corrected ($\Gamma = 0.4317$), maximum likelihood (ML) ($-\ln L = 7686.45$) GTR model with proportion of invariable sites (0.5179) on DNA alignments of 1842 (Nm) sites. Base frequencies and substitution rates were estimated with an ML search. Tree topology was determined using stepwise addition and 1 × heuristic searches with tree bisection-reconstruction (TBR) branch swapping and random-addition sequences. Numbers on branches correspond to bootstrap values (100 × with stepwise addition and a heuristic search with 2 × random addition and TBR branch swapping) for each ML tree.

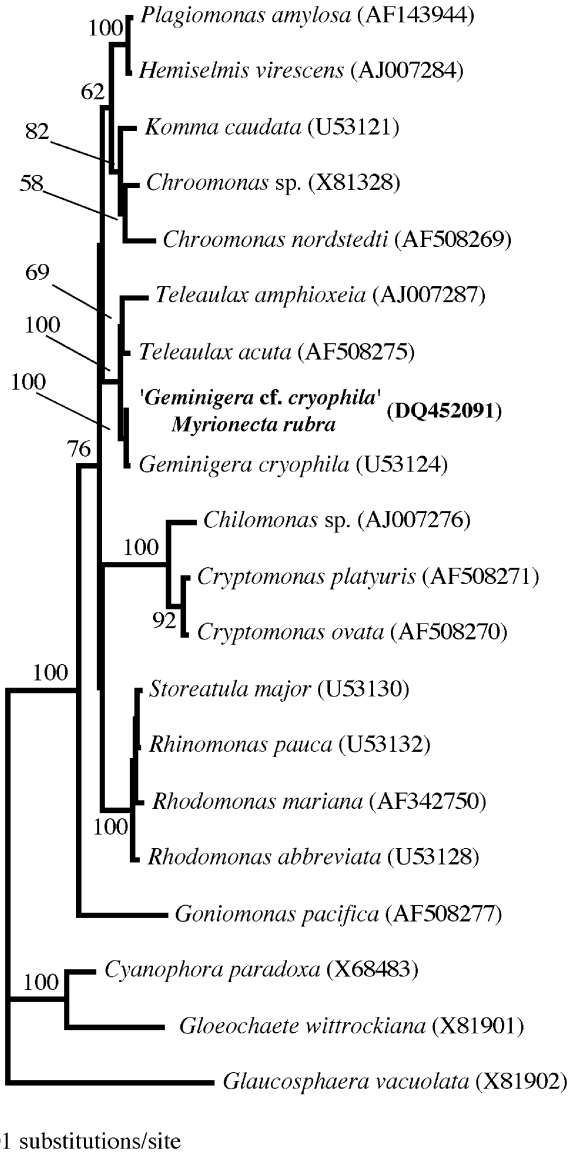

FIG. 2. Phylogenetic analysis of cryptophyte nuclear (Nu) small subunit rRNA genes for *Geminigera* cf. *cryophila* and *Myrionecta rubra* using a gamma-corrected ($\Gamma = 0.6326$), maximum likelihood (ML) ($-\ln L = 7339.95$) GTR model with proportion of invariable sites (0.4364) on DNA alignments 1829 (Nu) sites. Base frequencies and substitution rates were estimated with an ML search. Tree topology was found using stepwise addition and 1 × heuristic searches with tree bisection-reconstruction (TBR) branch swapping and random-addition sequences. Numbers on branches correspond to bootstrap values (100 × with stepwise addition and a heuristic search with 2 × random addition and TBR branch swapping) for each ML tree.

growth rates were not different between HL and LL (Table 2). Observations of thin sections of *M. rubra* using TEM revealed the presence of membrane-delineated chloroplast–mitochondrial complexes (CMCs), as described previously (Taylor et al. 1969, 1971, Hibberd 1977, Oakley and Taylor 1978) (Figs. 4 and 5). The chloroplasts possess a stalked pyrenoid, sometimes with two starch grains, and a Nm, surrounded by the periplastidal double membrane (Fig. 5). A single membrane surrounds the periplastidal unit, along with cryptophyte mitochondria (with flattened christae), cytoplasm, endoplasmic reticulum, and sometimes lipid droplets (Figs. 4 and 5). Chl *a* per cell was about six times greater in *M. rubra* than *G.* cf. *cryophila* on average, across all irradiance levels (Table 2). For both cultures, chl per cell did not differ at the two highest irradiance levels and increased at lower irradiance levels (Table 2). Carbon per cell was estimated based on cell volume (Menden-Deuer and Lessard 2000), yielding HL values of 564 ± 173 and 62.2 ± 8.5, and LL values of 561 ± 194 and 44.5 ± 7.4 for *M. rubra* and *G.* cf. *cryophila*, respectively. Chl-specific absorption spectra (a^{chl}) were essentially identical for both cultures within the visible spectral range, with a phycoerythrin peak at 550 nm (Fig. 6). However, in the UV portion of a^{chl}

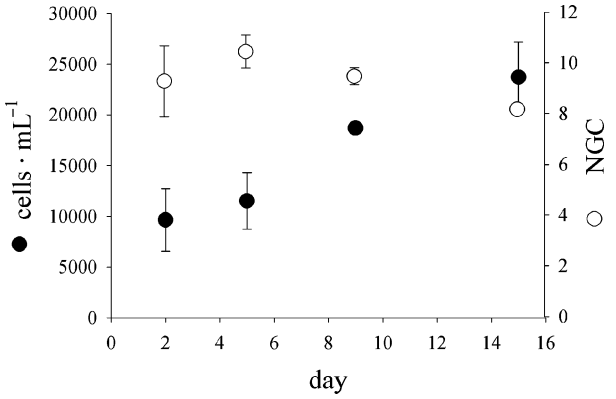

FIG. 3. Cell abundance and nucleomorph (Nm) genomes per cell (NGC) (~plastid number per cell) over time for a growing *Myrionecta rubra* culture. NGC estimated using quantitative (q) PCR with an assay designed for the *Geminigera* cf. *cryophila* Nm small subunit rRNA gene. All data points are mean ± standard deviation, $n = 3$.

FIG. 4. TEM section of *Myrionecta rubra* showing the chloroplast–mitochondria complex (CMC) harboring cryptophyte organelles. ER, endoplasmic reticulum; L, lipid droplet; M, cryptophyte mitochondria; NM, nucleomorph.

spectra, high and unexpected absorption at 335 nm (UVB) was found in *M. rubra*, absent in *G.* cf. *cryophila*, suggesting the production of mycosporine-like amino acids (MAA) in the ciliate (Fig. 6, Table 2).

Photophysiology. Maximum cellular photosynthetic rates (P^{cell}_{max}) for *M. rubra* were ~6–7.6 times greater than those for *G.* cf. *cryophila* (Table 2). For both *M. rubra* and *G.* cf. *cryophila*, P^{cell}_{max} increased with decreasing irradiance and chl concentration (Table 2). Maximum chl-specific photosynthetic rates (P^{chl}_{max}) were identical between cultures in both LL and HL (Table 2). Carbon-specific maximum photosynthetic rates were greater in *G.* cf. *cryophila* and increased for both cultures in LL (Table 2). Cell-specific carbon fixation efficiency (α^{cell}) increased with decreasing light for both taxa and were ~3–4 times greater in *M. rubra* (Table 2). Chl-specific carbon fixation efficiency (α^{chl}) was greater at all growth irradiances in *G.* cf. *cryophila*, as were measurements of photochem-

TABLE 2. Mean physiological parameters and SD in parentheses for *Myrionecta rubra* and *Geminigera* cf. *cryophila* in HL (75 and 90 µmol photons · m^{-2} · s^{-1}) and LL (10 and 25 µmol photons · m^{-2} · s^{-1}) at 5° C.

	Myrionecta rubra ($n = 3$)		*Geminigera* cf. *cryophila* ($n = 2$)		Ratios (MR:GC)	
	HL	LL[a]	HL	LL	HL	LL
C	564 (173)	561 (194)	62.2 (8.5)*	44.5 (7.4)*	9.07	12.6
µ	0.179 (0.03)	0.125 (0.034)	0.26 (0.02)***	0.20 (0.03) *	0.69	0.64
chl a · cell^{-1}	15.4 (2.8)	27.8 (5.9)	2.6 (0.14)***	4.5 (0.6)***	5.89	6.14
$a(p)^{chl\ 335}$	0.22 (0.08)	0.062 (0.015)	0.023 (0.002)***	0.018 (0.002)***	9.38	3.46
F_v/F_m	0.54 (0.04)	0.66 (0.01)	0.64 (0.02)**	0.73 (0.05) *	0.85	0.90
P^{cell}_{max}	10.1 (1.9)	21.9 (1.8)	1.7 (0.23)***	2.87 (0.24)**	5.95	7.61
P^{chl}_{max}	0.64 (0.16)	0.68 (0.04)	0.65 (0.07) NS	0.65 (0.13) NS	0.98	1.04
P^{c}_{max}	0.02 (0.005)	0.040 (0.003)	0.03 (0.006)**	0.065 (0.004)***	0.67	0.61
α^{cell}	0.16 (0.014)	0.394 (0.031)	0.04 (0.01)***	0.12 (0.04)***	4.02	3.40
α^{chl}	0.01 (0.001)	0.012 (0.001)	0.015 (0.004)**	0.025 (0.006)**	0.64	0.49
E_k	60.2 (9.9)	56.9 (3.5)	49.4 (2.7)	23.7 (7.8)***	1.22	2.41

[a]Twenty-five µmol photons · m^{-2} · s^{-1} only. Asterisks indicate results of a paired T-test analysis ($P<0.05$) between *M. rubra* and *G.* cf. *cryophila*.

*$P<0.05$.

**$P<0.005$.

***$P<0.001$.

NS, not significant; C = pg C · cell^{-1}; chl a · cell^{-1} = pg chl a · cell^{-1}; see Table 1 for descriptions and units of other parameters. LL, low light; HL, high light.

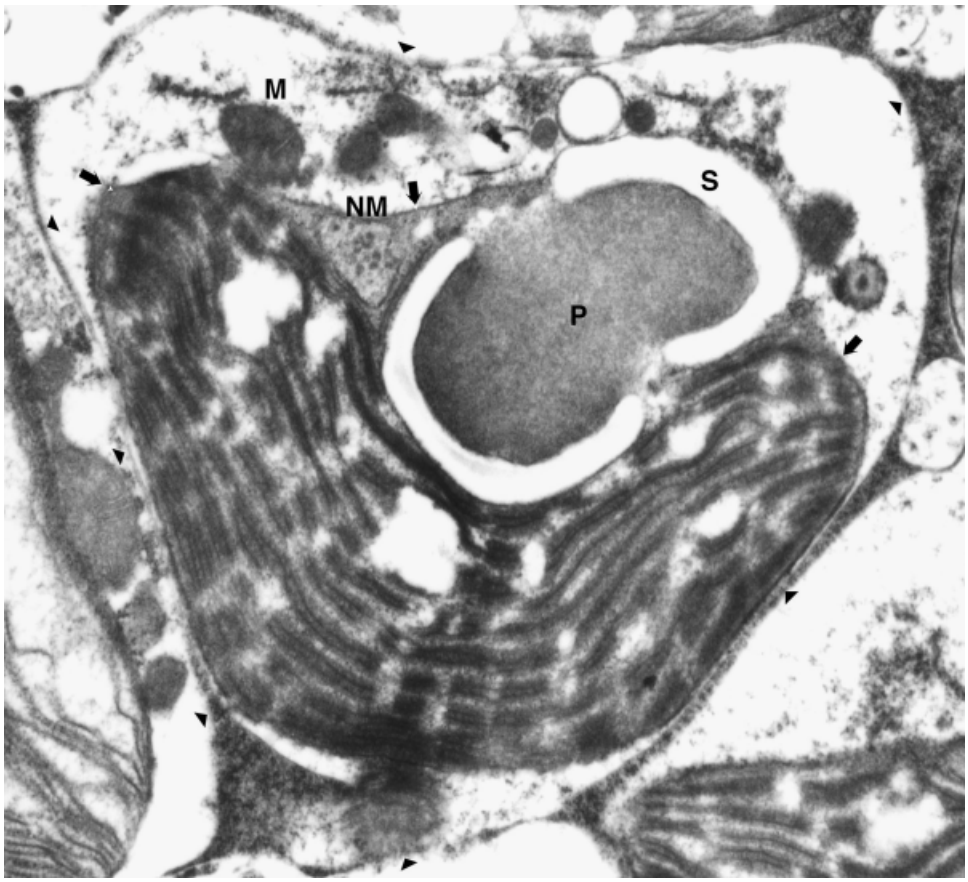

FIG. 5. TEM section of *Myrionecta rubra* showing the chloroplast–mitochondria complex (CMC) harboring cryptophyte organelles. M, cryptophyte mitochondria; NM, nucleomorph; P, pyrenoid; S, starch; long arrow, periplastidal double membrane; short arrow, CMC outer membrane.

ical efficiency (F_v/F_m) in HL (Table 2). Significant increases were seen in α^{chl} in the cryptophyte at lower irradiance levels ($P = 0.033$), while no change was observed in *M. rubra* (Table 2). The saturation irradiance parameter (E_k) was greater in *M. rubra* in LL, suggesting greater light-harvesting potential but poorer photochemical acclimation at low irradiance (Table 2).

Carbon partitioning. Lipid production in *M. rubra* was about 20% of total photosynthetic C production, compared with about 6% in *G.* cf. *cryophila* (Fig. 7a). Photosynthate-mediated protein synthesis was 31% greater in *G.* cf. *cryophila*, while low-molecular-weight compound (LMWC) and polysaccharide production were similar. The majority of fixed C in both cultures was found in the protein fraction, 64% and 44% for *G.* cf. *cryophila* and *M. rubra*, respectively. Comparisons of C partitioning were also made at three light levels for *M. rubra* only. In HL, *M. rubra* produced greater amounts of lipids and less protein, while more C remained in the polysaccharide pool in LL (Fig. 7b). No difference was observed in the LMWC fraction.

DISCUSSION

Plastid origin. We have shown that plastids in a cultured strain of *M. rubra* are phylogenetically identical to those of its prey, *G.* cf. *cryophila*, as all Nm SSU rRNA gene sequences amplified from the *M. rubra* and prey-only cultures were identical. These findings do not rule out the presence of another plastid type in *M. rubra*, including a permanent "symbiotic" plastid that could have been missed due to primer bias or existing in low concentrations. To further address this, quantitative PCR was used to determine if observed chl concentrations could be attributed to the *G. cryophila* plastid type by measuring Nm SSU rRNA gene concentration in growing *M. rubra* cells. Our *M. rubra* culture maintained eight to 10 *G.* cf. *cryophila* plastids per cell, and these plastids undergo division in growing *M. rubra*, as evidenced by measurements of Nm genomic copies of the SSU rRNA gene. Chl content in *M. rubra* has been shown to vary with feeding history (Gustafson et al. 2000, Johnson et al. 2004), and thus PNC is likely variable. While this is perhaps the first documentation of sequestered organelle division in a protist, the results are not surprising considering previous evidence for chl synthesis in this ciliate (Gustafson et al. 2000, Johnson and Stoecker 2005). These quantitative PCR estimates of plastids per cell agree reasonably well with estimates from ratios of chl per cell in *M. rubra* and free-living *G.* cf. *cryophila*, which can average between five and 12 plastids per cell for a population, depending on feeding history (estimated from

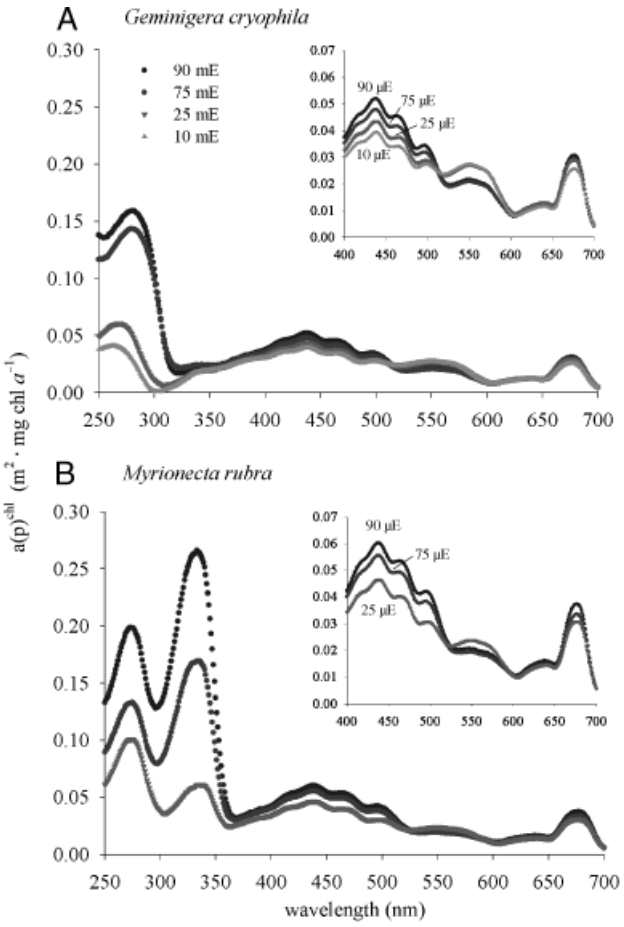

FIG. 6. UV and visible chl-specific spectral absorption for (A) *Geminigera* cf. *cryophila* and (B) *Myrionecta rubra*. Inset is visible spectrum only. All spectra are means ($n = 2$).

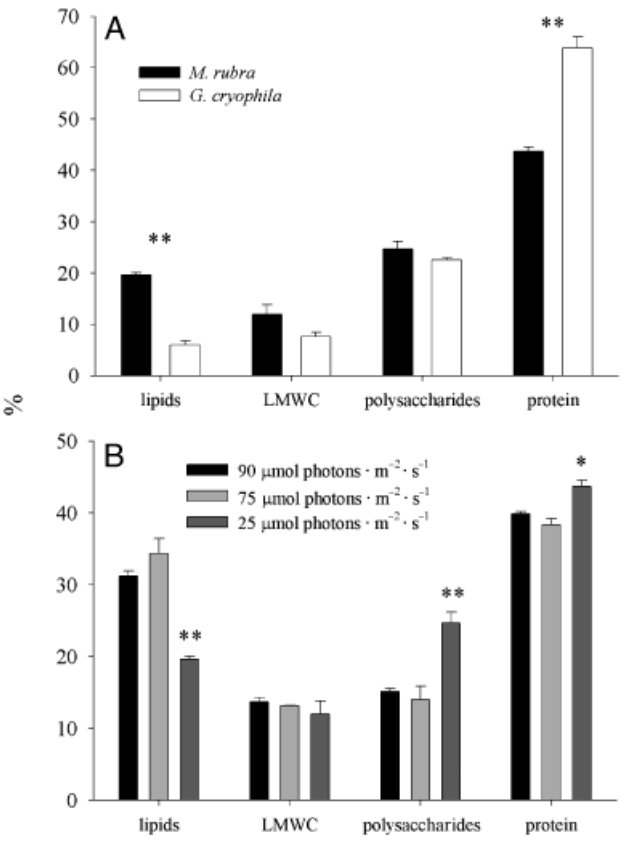

FIG. 7. Analysis of partitioning of photosynthetically fixed C into (A) *Geminigera* cf. *cryophila* and *Myrionecta rubra* acclimated to low light (25 µmol photons $\cdot m^{-2} \cdot s^{-1}$) and (B) *M. rubra* acclimated to low light and high light (75 and 90 µmol photons $\cdot m^{-2} \cdot s^{-1}$); $n = 3$; *T*-test: $^*P<0.05$, $^{**}P<0.01$.

Johnson and Stoecker 2005). While prolonged starvation of *M. rubra* from *G. cryophila* prey results in dramatic decline of chl per cell, cells stop growing or die before losing all chl (Johnson and Stoecker 2005).

Individual cell variability for plastid content in *M. rubra* is certainly much greater than the numbers presented above, as both unusually large and small cells are frequently observed within the culture. Our plastid per cell data are similar to those of Hibberd (1977), who estimated 12 CMCs per cell, while other estimates far outnumber those presented here. Oakley and Taylor (1978) estimated 50–100 CMCs per cell in populations of large *M. rubra* in British Columbia, while Fenchel (1968) estimated 10–20 in cells collected in the Isefjord of Denmark. In the Baltic Sea, distinct size classes of co-occurring large and small *M. rubra* are well known (Lindholm 1978, Rychert 2004), yet it is unclear if this is due to differences in division rate, life history stages, or undescribed species variation. The ultrastructure of CMCs in the *M. rubra* culture is consistent with those described elsewhere, with the plastid and Nm intact within the periplastidal membrane complex, together with cryptophyte mitochondria, cytoplasm, and endoplasmic reticulum enclosed within a single membrane (Taylor et al. 1969, 1971; Hibberd 1977; Oakley and Taylor 1978). Clearly the degree of phenotypic variability described for *M. rubra* and its "symbionts" warrants comparative ultrastructural and molecular analyses to determine if it is truly a single species or a complex of closely related species.

Photosynthetic physiology. M. rubra plastids are used in an independent fashion, with optimal performance and sustained maintenance dependent on recurrent feeding (Johnson and Stoecker 2005). Comparison of photosynthetic physiology between *M. rubra* and its prey *G.* cf. *cryophila* revealed several important differences. In HL, plastids in *G.* cf. *cryophila* have greater photosynthetic efficiency (i.e. α^{chl}) and optimal quantum efficiency (F_v/F_m), suggesting differences in plastid packaging, repair mechanisms, and/or energy dissipation. However, P^{chl}_{max} rates were about the same between cultures, indicating similar capacity for photosynthesis under saturating irradiance. Lower F_v/F_m in *M. rubra* indicates a slight loss of absorbed energy. Differences in quantum efficiency between the two cultures could be explained by differential abundance of important electron transport chain proteins, differences in nitrogen assimilatory pathways, or other factors that

may affect the flow of electrons through plastoquinone (Falkowski and Raven 1997).

While higher measurements of P^{chl}_{max} have been observed previously for this *M. rubra* culture (up to 1.5 pg C · pg chl $a^{-1} \cdot h^{-1}$), photosynthetic performance of *M. rubra* depends greatly on recent feeding history, increasing as cells become starved and chl *a* per cell declines (Johnson and Stoecker 2005). Satoh and Watanabe (1991) measured similar P^{chl}_{max} rates (1.04 pg C · pg chl $a^{-1} \cdot h^{-1}$) for *M. rubra* in Antarctic waters. While our measurements for P^{chl}_{max} in *G.* cf. *cryophila* and *M. rubra* are low for phytoplankton, they fall well within the range of measured polar microalgae, which generally varies between 0.3 and 2.0 pg C · pg chl $a^{-1} \cdot h^{-1}$ (Sakshaug and Slagstad 1991, Robinson et al. 1997). It is generally thought that low temperature limits the activity of carbon fixation enzymes (e.g. RUBISCO), thus limiting photosynthesis (Berry and Bjorkman 1980).

One major difference observed between cultures was the absorbance of compounds in *M. rubra* that resemble MAA, absent in the *G.* cf. *cryophila* culture (Fig. 6). The MAAs have been shown to protect against UV inhibition of photosynthesis in *Akashiwo sanguinea* (= *Gymnodinium sanguineum*) (Neale et al. 1998), and have been reported in diverse phytoplankton lineages (Jeffrey et al. 1999) including ciliates (Tartarotti et al. 2004). In *M. rubra*, MAA production increased with increasing E_g, suggesting that irradiance levels induce MAA production, as is found in *A. sanguinea* (Neale et al. 1998). Perhaps the presence of MAAs in *M. rubra* helps to explain their propensity to form surface-oriented red tides, while their absence in cryptophytes explains the lack of surface accumulations in this group.

In phytoplankton, α^{chl} generally does not vary phenotypically (e.g. with acclimation state), and variation among taxa can be attributed to differences in pigment composition and packaging (MacIntyre et al. 2002). Chl-specific photosynthetic efficiency (α^{chl}) for *M. rubra* did not change between HL and LL in this study and was significantly lower than for *G.* cf. *cryophila* at all light levels. Lower α^{chl} in *M. rubra* is likely because of a "packaging effect," where absorption of light per unit chl *a* is less efficient due to high chl *a* per cell concentration. Surprisingly, α^{chl} did change for *G.* cf. *cryophila* by increasing in LL, suggesting that changes in α^{chl} may be due to something other than chl *a* concentration. In cyanobacteria, α^{chl} increases with decreasing E_g due to increases in phycobilin concentration, as phycobilins are the major light-harvesting pigment in cyanobacteria (Kana and Glibert 1987). In cryptophytes, however, this is generally thought not to be the case (Adolf et al. 2003), and thus changes in α^{chl} reported here for *G.* cf. *cryophila* might be due to changes in pigment packaging or optical qualities of the cell. Based on measurements of saturation irradiance (E_k), neither *M. rubra* nor *G.* cf. *cryophila* were exposed to saturating growth irradiance in LL. Previous research with *M. rubra* suggests that in HL, E/E_k is greater than 1 following feeding and declines during starvation as cells lose the ability to make chl *a* and essentially become light limited (Johnson and Stoecker 2005). While *M. rubra* functions like a phototroph and is capable of temporary chl *a* synthesis (Gustafson et al. 2000, Johnson and Stoecker 2005), it may not be able to photoacclimate to E_g as efficiently as other phototrophs.

Growth and Carbon metabolism. *M. rubra* is well known for its ability to generate red tides and its high photosynthetic rates (Smith and Barber 1979). Thus measurements for P and μ presented here and elsewhere (Gustafson et al. 2000, Johnson and Stoecker 2005) for this Antarctic strain of *M. rubra* appear quite modest. Recently, Yih et al. (2004) found maximum growth for a strain of *M. rubra* growing at 15° C to be 0.521 d^{-1}. Using maximum growth rates observed for the Antarctic strain (~0.2 d^{-1}) at 5° C, this would suggest a Q_{10} of about 2.6, which is similar to median Q_{10} values for respiration rates in protists (Caron et al. 1990). The Q_{10} for photosynthesis in microalgae for temperatures within the 2–8° C range is generally around 3 (Palmisano et al. 1987). Thus, using data presented here and elsewhere (Johnson and Stoecker 2005), one may expect that *M. rubra* growing at 15° C would have a P^{chl}_{max} between 3 and 5 pg C · pg chl $a^{-1} \cdot h^{-1}$, which is more consistent with measurements of Stoecker et al. (1991) who measured 1.8–8.6 pg C · pg chl $a^{-1} \cdot h^{-1}$ at temperatures between 15 and 22° C in temperate populations of *M. rubra*.

Differences in P^{cell}_{max} rates for *M. rubra* and *G.* cf. *cryophila* scaled with observed differences in chl *a* per cell with values for *M. rubra* being ~6-fold greater. Averaged μ for *M. rubra* was 62.6 ± 6.6% of *G.* cf. *cryophila*, which agreed well with observed P^{C}_{max} rates (64.8 ± 4.2% of *G.* cf. *cryophila*) and θ ratios (57.9 ± 11% of *G.* cf. *cryophila*) across all irradiance levels (E_g). The Chl:C ratio is a key physiological parameter, as chl *a* and C are widely used to normalize photosynthetic rates (MacIntyre et al. 2002). Lower θ quotas in *M. rubra* are probably the major cause of lower μ for *M. rubra*, as both P^{chl}_{max} and P^{C}_{max} rates were greater in *G.* cf. *cryophila*. Johnson and Stoecker (2005) demonstrated that μ in *M. rubra* is ultimately limited by availability of *G.* cf. *cryophila* prey, but declines slowly during periods of prolonged starvation, despite the presence of inorganic nutrients and somewhat sustained photosynthetic rates. Therefore, in *M. rubra* θ, μ and to a lesser extent P are sensitive to prior feeding history. Variable prey concentrations were not controlled in this study and thus their effect on photosynthetic rates and μ in *M. rubra* cannot be evaluated here. Growth rates presented here for *M. rubra* are similar to previous observations for this culture (~0.19 d^{-1}) (Johnson and Stoecker 2005), as well as to values reported for *M. rubra* in brackish Antarctic lakes (~0.18 d^{-1}; Laybourn-Parry et al. 2000). Growth for HL *G.* cf. *cryophila* (~0.26 d^{-1}) was substantially higher than for *M. rubra*, and higher than for cryptophytes in brackish Antarctic lakes (~0.08–0.14 d^{-1}; Laybourn-

Parry et al. 2000). However, comparisons of *G.* cf. *cryophila* growth at close to *in situ* irradiance levels for Antarctic Lakes (3.5–13 μmol photons $\cdot m^{-2} \cdot s^{-1}$) reveal similar rates (Marshall and Laybourn-Parry 2002). Likewise, the P_{max}^{cell} values for *G.* cf. *cryophila* acclimated to 10 μmol photons $m^{-2} \cdot s^{-1}$ reveal values similar to those reported for Lake Fryxell (~1.3 pg $C \cdot cell^{-1} \cdot h^{-1}$; Marshall and Laybourn-Parry 2002).

Calculations of the percentage of growth per day (as C) attributable to photosynthesis indicate that in HL *M. rubra* and *G.* cf. *cryophila* both fix similar proportions of new C per day (~147% cell $C \cdot d^{-1}$), while in LL *G.* cf. *cryophila* fixes proportionately 35% more C (256% and 189% cell $C \cdot d^{-1}$, for *G.* cf. *cryophila* and *M. rubra*, respectively). In order to compare *M. rubra* to other plastid-sequestering protists, we calculated phototrophic C production for the plastidic oligotrich *Laboea strobila* (Stoecker et al. 1988) and the kleptoplastidic dinoflagellate *Gymnodinium 'gracilentum'* (Skovgaard 1998). While *L. strobila* has high P_{max}^{chl} rates, photosynthetically fixed C only accounts for 19.7% of new cell C per day. *Gymnodinium 'gracilentum'* was found to fix a greater proportion of cell C (83.3%), but still requires substantial heterotrophic C assimilation to meet growth and respiration requirements. Calculations for percentage of new C fixed per day for *M. rubra* in this study and previous observations (Johnson and Stoecker 2005) varied between 148% and 263% d^{-1} and are similar to other phototrophs.

Comparisons of C partitioning in major biochemical fractions in microalgal cultures and phytoplankton assemblages has been used to infer mechanisms of C storage, major differences in C metabolism between taxa, and to evaluate effects of nutrient limitation (Morris 1981). Our results suggest that *M. rubra* stores high quantities of fixed C as lipids, which increases in HL. While both *M. rubra* and *G.* cf. *cryophila* produced large quantities of protein, greater protein production in *G.* cf. *cryophila* may simply reflect higher growth rates. Putt (1990) compared C partitioning of retained plastids in the photosynthetic oligotrich ciliate *L. strobila* to those of prey and found that proportionately less C from photosynthesis in *L. strobila* was used for production of protein and lipids, while more remained within the polysaccharide fraction. Thus photosynthesis in *L. strobila*, and presumably other plastidic oligotrichs, is primarily used to cover respiratory costs (Putt 1990). Our calculation of C production per day for *L. strobila* (above) also supports the notion that plastidic oligotrichs have high heterotrophic C requirements. *M. rubra* appears to have little need for heterotrophic C, and while growth is optimal following feeding on cryptophytes, it appears to be a result of enhanced growth efficiency and phototrophy (Johnson and Stoecker 2005). Estimates of heterotrophic C contribution to the C budget of *M. rubra* indicate that feeding accounts for an insignificant amount of growth, suggesting that the need for periodic ingestion of prey is simply to replenish cryptophyte organelles (Gustafson et al. 2000, Yih et al. 2004, Johnson and Stoecker 2005). Differences in lipid production between *M. rubra* and *G.* cf. *cryophila* may reflect differences in membrane structures or variation in the extent and form of storage products. High production of lipids in algal cells has also been attributed to N limitation and adaptation to living in polar ice (Kirst and Wiencke 1995).

CONCLUSIONS

We have shown that *M. rubra* functions as a proficient phototroph, using plastids from *G.* cf. *cryophila* in a commensurately efficient manner in HL but not LL conditions. Major differences in growth rates observed between *M. rubra* and *G.* cf. *cryophila* were best explained by differences in θ and P_{max}^{C} rates, both of which vary with feeding history in *M. rubra*. High protein and lipid production from photosynthate suggests that plastids are integrated into biosynthetic pathways of *M. rubra*, unlike other plastid-retaining protists. The division of sequestered plastids is a unique characteristic, indicating that *M. rubra* has regulatory control over chl synthesis and plastid division. This and previous studies of *M. rubra* (Gustafson et al. 2000, Johnson et al. 2004, Johnson and Stoecker 2005) suggest that the ciliate may be in the transition of permanently acquiring plastids, and thus serves as a useful evolutionary model for tertiary plastid acquisition via organelle retention. It is important that future studies of the ciliate begin to focus on strain and/or species variation with feeding and "symbiont" organization.

We thank J. Adolf, T. Kana, D. W. Coats, and C. Delwiche for comments on this manuscript and D. Gustafson for technical assistance during the project. Additional thanks to T. Kana for use of his PAM fluorometer. This material is based on work supported by the National Science Foundation under Grant No. 0131847. UMCES contribution number 4008.

Adolf, J. E., Stoecker, D. K. & Harding Jr., L. W. 2003. Autotrophic growth and photoacclimation in *Karlodinium micrum* (Dinophyceae) and *Storeatula major* (Cryptophyceae). *J. Phycol.* 39:1101–8.

Berry, J. & Bjorkman, O. 1980. Photosynthetic response and adaptation to temperature in higher plants. *Annu. Rev. Plant Physiol.* 31:491–543.

Caron, D. A., Goldman, J. C. & Fenchel, T. 1990. Protozoan respiration and metabolism. *In* Capriulo, G. M. [Ed.] *Ecology of Marine Protozoa*. Oxford University Press, New York, pp. 307–22.

Crawford, D. W., Purdie, D. A., Lockwood, A. P. M. & Weissman, P. 1997. Recurrent red-tides in the Southampton Water Estuary by the phototrophic ciliate *Mesodinium rubrum*. *Estuar. Coast. Shelf Sci.* 45:799–812.

Falkowski, P. G. & Raven, J. A. 1997. *Aquatic Photosynthesis*. Blackwell, Malden.

Frenchel, T. 1968. On "red water" in the Isefjord (inner Danish waters) caused by the ciliate *Mesodinium rubrum*. *Ophelia* 5: 245–53.

Gillott, M. A. & Gibbs, S. P. 1980. The cryptophyte nucleomorph: its ultrastructure and evolutionary significance. *J. Phycol.* 16:558–68.

Guillard, R. R. L. 1975. Culture of phytoplankton for feeding marine invertebrates. *In* Smith, W. L. & Chanley, M. H. [Eds.] *Cuture of Marine Invertebrate Animals*. Plenum Publishing, New York, pp. 29–60.

Gustafson, D. E., Stoecker, D. K., Johnson, M. D., Van Heukelem, W. F. & Sneider, K. 2000. Cryptophyte algae are robbed of their organelles by the marine ciliate *Mesodinium rubrum*. *Nature* 405:1049–52.

Hibberd, D. J. 1977. Observations on the ultrastructure of the cryptomonad endosymbiont of the red water ciliate *Mesodinium rubrum*. *J. Mar. Biol. Assoc. UK* 57:45–61.

Hill, D. R. A. 1991. A revised circumscription of *Cryptomonas* (Cryptophyceae) based on examination of Australian strains. *Phycologia* 30:170–88.

Hoef-Emden, K., Marin, B. & Melkonian, M. 2002. Nuclear and nucleomorph SSU rDNA phylogeny in the cryptophyta and the evolution of cryptophyte diversity. *J. Mol. Evol.* 55: 161–79.

Jankowski, A. W. 1976. Revision of the classification of the cyrtophorids. *In* Markevich, A. P. & Yu, I. [Eds.] *Materials of the II All-Union Conference of Protozoology Part I, General Protozoology.* Naukova Dumka, pp. 167–8.

Jeffrey, S. W., MacTavish, H. S., Dunlap, W. C., Vesk, M. & Groenewoud, K. 1999. Occurrence of UVA- and UVB-absorbing compounds in 152 species (206 strains) of marine microalgae. *Mar. Ecol. Prog. Ser.* 189:35–51.

Johnson, M. D. & Stoecker, D. K. 2005. The role of feeding in growth and the photophysiology of *Myrionecta rubra*. *Aquat. Microb. Ecol.* 39:303–12.

Johnson, M. D., Tengs, T., Oldach, D. W., Delwiche, C. F. & Stoecker, D. K. 2004. Highly divergent SSU rRNA genes found in the marine ciliates *Myrionecta rubra* and *Mesodinium pulex*. *Protist* 155:347–59.

Kana, T. M. & Glibert, P. M. 1987. Effect of irradiances up to $2000\,\mu E\,m^{-2}s^{-1}$ on marine *Synechococcus* WH7803: I. Growth, pigmentation, and cell composition. *Deep-Sea Res.* 34:479–95.

Kirst, G. O. & Wiencke, C. 1995. Ecophysiology of polar algae. *J. Phycol.* 31:181–99.

Kishino, M., Takahashi, M., Okami, N. & Ichimura, S. 1985. Estimation of the spectral absorption coefficients of phytoplankton in the sea. *Bull. Mar. Sci.* 37:634–42.

Laybourn-Parry, J., Bell, E. M. & Roberts, E. C. 2000. Protozoan growth rates in Antarctic Lakes. *Polar Biol.* 23:445–51.

Lewis, M. R. & Smith, J. C. 1983. A small volume, short-incubation-time method for measurement of photosynthesis as a function of incident irradiance. *Mar. Ecol. Prog. Ser.* 13:99–102.

Lewitus, A. J., Glasgow, H. B. & Burkholder, J. M. 1999. Kleptoplastidy in the toxic dinoflagellate *Pfiesteria piscicida* (Dinophyceae). *J. Phycol.* 35:303–12.

Lindholm, T. 1978. Autumnal mass development of the "red water" ciliate *Mesodinium rubrum* in the Åland archipelago. *Memo. Soc. Fauna Flora Fenn.* 54:1–5.

Lindholm, T. 1985. *Mesodinium rubrum*—a unique photosynthetic ciliate. *Adv. Aquat. Microbiol.* 3:1–48.

MacIntyre, H. L., Kana, T. M., Anning, T. & Geider, R. 2002. Photoacclimation of photosynthesis irradiance response curves and photosynthetic pigments in microalgae and cynaobacteria. *J. Phycol.* 38:17–38.

Maddison, W. P. & Maddison, D. R. 1992. *MacClade: Analysis of Phylogeny and Character Evolution*. Sinauer, Sunderland, Massachusetts.

Marshall, W. & Laybourn-Parry, J. 2002. The balance between photosynthesis and grazing in Antarctic mixotrophic cryptophytes during summer. *Freshw. Biol.* 47:2060–70.

Medlin, L., Elwood, H. J., Stickel, S. & Sogin, M. L. 1988. The characterization of enzymatically amplified eukaryotic 16S-like rRNA-coding regions. *Gene* 71:491–99.

Menden-Deuer, S. & Lessard, E. J. 2000. Carbon to volume relationships for dinoflagellates, diatoms, and other protist plankton. *Limnol. Oceanogr.* 45:569–79.

Morris, I. 1981. Photosynthesis products, physiological state, and phytoplankton growth. *In*: Platt T [Ed.] *Physiological Basis of Phytoplankton Ecology. Can. Bull. Fish. Aquat. Sci.* 210: 83–102.

Morris, I., Glover, H. E. & Yentsch, C. S. 1974. Products of photosynthesis by marine phytoplankton: the effect of environmental factors on the relative rates of protein synthesis. *Mar. Biol.* 27:1–9.

Neale, P. J., Banaszak, A. T. & Jarriel, C. R. 1998. Ultraviolet sunscreens in *Gymnodinium saunguineum* (Dinophyceae): mycosporine-like amino acids protect against inhibition of photosynthesis. *J. Phycol.* 34:928–38.

Oakley, B. R. & Taylor, F. J. R. 1978. Evidence for a new type of endosymbiotic organization in a population of the ciliate *Mesodinium rubrum* from British Columbia. *Biosystems* 10: 361–9.

Oldach, D. W., Delwiche, C. F., Jakobsen, K. S., Tengs, T., Brown, E. G., Kempton, J. W., Schaefer, E. F., Bowers, H. A., Glasgow, H. B. Jr., Burkholder, J. M., Steidinger, K. A. & Rublee, P. A. 2000. Heteroduplex mobility assay-guided sequence discovery: elucidation of the small subunit (18S) rDNA sequences of *Pfiesteria piscicida* and related dinoflagellates from complex algal cultures and enviromental sample DNA pools. *PNAS* 97: 4303–8.

Palmisano, A. C., Smith, G. A., White, D. C., Nichols, P. D., Lizotte, M. P., Cota, G. & Sullivan, C. W. 1987. Changes in photosynthetic metabolism in sea-ice microalgae during a spring bloom in McMurdo Sound. *Antarct. J.* 22:176–7.

Parsons, T. R., Maita, Y. & Lalli, C. M. 1984. *A Manual of Chemical and Biological Methods for Seawater Analysis*. Pergamon Press, Oxford.

Platt, T., Gallegos, C. L. & Harrison, W. G. 1980. Photoinhibition of photosynthesis in natural assemblages of marine phytoplankton. *J. Mar. Res.* 38:687–701.

Putt, M. 1990. Metabolism of photosynthate in the chloroplast-retaining ciliate *Laboea strobila*. *Mar. Ecol. Prog. Ser.* 60: 271–82.

Robinson, D. H., Kolber, Z. & Sullivan, C. W. 1997. Photophysiology and photoacclimation in surface sea ice algae from McMurdo Sound, Antarctica. *Mar. Ecol. Prog. Ser.* 147: 243–56.

Rychert, K. 2004. The size structure of the *Mesodinium rubrum* population in the Gdansk Basin. *Oceanologia* 46:439–44.

Ryther, J. H. 1967. Occurrence of red water off Peru. *Nature* 214:1318–9.

Sakshaug, E. & Slagstad, D. 1991. Light and productivity of phytoplankton in polar marine ecosystems: a physiological view. *In*: Sakshaug, E., Hopkins, C.C.E. and Oritsland, N.A. [Eds.] *Proceedings of the Pro Mare Symposium on Polar Marine Ecology. Polar Res.* 10:69–85.

Satoh, H. & Watanabe, K. 1991. A red-water bloom caused by the autotrophic ciliate, *Mesodinium rubrum*, in the austral summer in the fast ice area near Syowa station, Antarctica, with note on their photosynthetic rate. *J. Tokyo Univ. Fish.* 78: 11–17.

Skovgaard, A. 1998. Role of chloroplast retention in a marine dinoflagellate. *Aquat. Microb. Ecol.* 15:293–301.

Smith, W. O. Jr. & Barber, R. T. 1979. A carbon budget for the autotrophic ciliate *Mesodinium rubrum*. *J. Phycol.* 15:27–33.

Stoecker, D. K., Putt, M., Davis, L. H. & Michaels, A. E. 1991. Photosynthesis in *Mesodinium rubrum*: species-specific measurements and comparison to community rates. *Mar. Ecol. Prog. Ser.* 73:245–52.

Stoecker, D. K. & Silver, M. W. 1990. Replacement and aging of chloroplasts in *Strombidium capitatum* (Ciliophora: Oligotrichida). *Mar. Biol.* 107:491–502.

Stoecker, D. K., Silver, M. W., Michaels, A. E. & Davis, L. H. 1988. Obligate mixotrophy in *Laboea strobila*, a ciliate which retains chloroplasts. *Mar. Biol.* 99:415–23.

Swofford, D. L. 1999. *PAUP*: Phylogenetic Analysis Using Parsimony.* Sinauer, Sunderland, Massachusetts.

Tartarotti, B., Baffico, G., Temporetti, P. & Zagarese, H. E. 2004. Mycosporine-like amino acids in planktonic organisms living under different UV exposure conditions in Patagonian lakes. *J. Plankton Res.* 26:753–62.

Taylor, D. L. & Lee, C. C. 1971. A new cryptomonad from Antarctica: *Cryptomonas cryophila* sp. nov. *Arch. Microbiol.* 75:269–80.

Taylor, F. J. R., Balckbourn, D. J. & Blackbourn, J. 1969. Ultrastructure of the chloroplasts and associated structures within

the marine ciliate *Mesodinium rubrum* (Lohmann). *Nature* 224:819–21.

Taylor, F. J. R., Blackbourn, D. J. & Blackbourn, J. 1971. The red-water ciliate *Mesodinium rubrum* and its "incomplete symbionts": a review including new ultrastructural observations. *J. Fish. Res. Board Canada* 28:391–407.

Thompson, J. D., Gibson, T. J., Plewniak, F., Jeanmougin, F. & Higgins, D. G. 1997. The CLUSTAL_X windows interface: flexible strategies for multiple sequence alignment aided by quality analysis tools. *Nucleic Acids Res.* 25:4876–82.

Yih, W., Kim, H. S., Jeong, H. J., Myung, G. & Kim, Y. G. 2004. Ingestion of cryptophyte cells by the marine photosynthetic ciliate *Mesodinium rubrum*. *Aquat. Microb. Ecol.* 36:165–70.